

Single metafilm effective medium behavior in optical domain: Maxwell-Garnett approximation and beyond

Natalia Dubrovina¹, Loïc O. Le Cunff³, N. Burokur¹, R. Ghasemi¹, A. Degiron^{1,2}, A. De Lustrac¹,
A. Vial³, G. Lerondel³, and A. Lupu^{1,2}

¹Univ. Paris-Sud, Institut d'Electronique Fondamentale, UMR 8622, 91405 Orsay Cedex, France

²CNRS, Orsay, F-91405, France

³Laboratoire de Nanotechnologie et d'Instrumentation Optique, Institut Charles Delaunay, Université de Technologie de Troyes, 12 rue Marie Curie, BP 2060, 10010 Troyes Cedex, France

*corresponding author: anatole.lupu@u-psud.fr

Abstract

It is empirically shown by numerical modeling that a single metafilm formed by an array of cut wires on a Silicon substrate behaves like a homogeneous layer for normal or oblique incidence.

1. Introduction

Metamaterials (MMs) have generated a lot of interest during the last decade due to their ability to provide unusual electromagnetic behavior, not encountered in natural materials [1,2]. They are commonly obtained by an implementation of a periodical arrangement of resonant elements, called also meta-atoms. Both the periodicity and the size of resonant elements are typically much smaller than the wavelength. This feature makes it possible to model their properties using an approach similar to that used for continuous media in classical electrodynamics or optics.

In this approach, MMs are treated as bulk effective media with a certain thickness and associated dielectric permittivity ϵ and magnetic permeability μ that are anisotropic in the most general case.

This approach proved to be valid, but essentially in the microwave domain [3]. Difficulties arise in the optical domain, in particular for the most common case of a single metafilm on a dielectric substrate. As mentioned by several authors [3-7], it is not clear whether the effective medium approach is valid for describing single metafilm behavior and what thickness should be assigned to the MMs in this case.

A few attempts to provide an answer to this question were done in [8,9]. In [9] the behavior of a metafilm formed by gold nanowires and split ring resonators (SRRs) was investigated by Fourier transform infrared (FTIR) experiments in the mid IR domain. By exploiting the interferogram of the asymmetric cavity formed by the metafilm and the silicon substrate and the zero order of transmission of the silicon/metamaterial phase mask, it was

shown that an effective index of refraction could be indeed assigned to the metafilm around the first plasmonic resonance of SRRs. However since this kind of interferometric measurements is sensitive to the optical length difference, the question of unambiguous determination of a metafilm effective index and thickness remains still open.

This paper aims at providing an answer to this question and to demonstrate that in the limit of Maxwell-Garnett (M-G) effective medium model, the behavior of a single metafilm on a substrate can be approximated by that of a homogeneous layer with a thickness equal to that of the deposited metal.

2. Single metafilm modeling and effective medium behavior validity criteria

For our study we consider the example of an array of gold cut wires (CWs) on a Silicon substrate. It represents probably the most elementary type of MMs used for building more complex geometry MMs. Its greatest advantage is the essentially non-magnetic behavior with $\mu \approx 1$ due to the absence of notable coupling between the electrical and magnetic resonances.

To prove that such a CW meta-surface can be indeed described as a homogeneous layer, it is necessary to verify that its behavior meets the following conditions:

- Effective magnetic permeability $\mu \approx 1$, except near the resonance region (non-magnetic behavior).
- Linearity of the dielectric permittivity variation with MMs surface filling factor ρ (validity of (M-G) approximation).
- Linearity of the optical length variation with respect to the deposited metal thickness).
- Invariance of the MMs layer dielectric permittivity with respect to the incidence angle variation

The phase and amplitude transmission and reflection modeling of an array of gold cut wires (CWs) on a Silicon substrate is performed by means of HFSS software from

Ansoft [10] and finite difference time domain (FDTD) modeling [11]. The dielectric permittivity of Au used for numerical modeling is that given by Palik [12]. For the sake of simplicity we consider a substrate with a refractive index of 3.45 that doesn't vary with the wavelength. This index value is that of the silicon at 1.5 μ m. To calculate the metafilm effective permittivity ϵ_{eff} and permeability μ_{eff} from the complex reflection and transmission coefficients r and t , respectively, we use the retrieval method detailed in [13], derived in much the same way as in [6].

The refraction index of a metafilm of thickness h is:

$$n_{\text{eff}} = \sqrt{\left(\frac{\beta}{k_0 h}\right)^2 + n_i^2 \sin^2 \theta_i} \quad (1)$$

$$\text{Here } \beta = \pm \arccos(\cos \beta) + \frac{2\pi m}{k_0 h} \quad (2)$$

where m is an integer. The explanation about the proper choice of the sign and value of the integer coefficient m can be found in [14].

In its turn:

$$\cos \beta = \frac{\sqrt{p_1 p_l}}{p_l (1-r) + p_l (1+r)} \frac{(1-r^2 + t'^2)}{t'} \quad (3)$$

$$\text{where } p = \sqrt{\frac{\epsilon}{\mu}} \cos \theta = \frac{1}{z} \cos \theta \quad (4)$$

is the medium characteristic admittance, i.e. the inverse of the medium impedance z for polarization perpendicular to the incidence plane. The index 1 and l designate first and last semi-infinite media. The metafilm layer impedance z_{eff} is used for calculating $\epsilon_{\text{eff}} = n_{\text{eff}}^2 / z_{\text{eff}}$ and $\mu_{\text{eff}} = n_{\text{eff}}^2 \cdot z_{\text{eff}}$:

$$z_{\text{eff}}^2 = \frac{1}{\cos^2(\theta_{\text{eff}})} \frac{\frac{1}{p_l} \cos \beta - \frac{1}{\sqrt{p_1 p_l}} \frac{1+r}{t'}}{p_l \cos \beta - \sqrt{p_1 p_l} \frac{1-r}{t'}} \quad (5)$$

$$\text{where } \cos \theta_{\text{eff}} = \sqrt{1 - \left(\frac{n_i}{n_{\text{eff}}}\right)^2 \sin^2 \theta_i} \quad (6)$$

The obtained results were used to verify the introduced above effective medium validity criteria. For this the numerical modeling detailed below was performed.

2.1. Metafilm thickness determination

The first point of our analysis concerns the determination of the thickness to be assigned to the metafilm. As mentioned, outside the resonance region, the effective permeability obtained by the retrieval procedure must be consistent with the condition $\mu \approx 1$ [14].

In the (M-G) approximation the MMs layer represents a mixture of CWs and air. Here we make the hypothesis that its thickness h equals that of the deposited metal. To verify this assertion, HFSS numerical modeling was performed for CWs with several metal thicknesses ranging from 20nm to 100nm. The length of the CWs is fixed to 200nm and its width to 50nm. The separation distance between adjacent CWs in transverse and longitudinal directions is 250nm and 100nm, respectively. The related filling factor p , defined as the fraction of the surface occupied by the MMs is 11% and

corresponds to the case of a weak coupling interaction between the CWs.

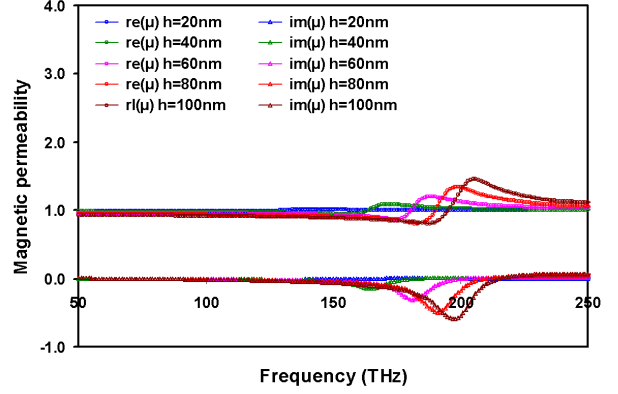


Figure 1: Real and imaginary parts of magnetic permeability μ obtained for different metal thickness CW array.

The results obtained for normal incidence with electric field orientation along the longitudinal CWs axis are displayed Fig. 1. It can be seen that outside the resonance region the condition $\mu \approx 1$ is well satisfied in the whole range of metal thickness variation, thus validating our hypothesis about the thickness of the effective layer. The region where μ differs from unity corresponds to the well-known magnetic antiresonance that is always concomitant with the electric resonance [15].

The shift toward higher frequencies of the resonance when metal thickness is increased is likely to be related to the decrease of the asymmetric bound supermode effective index [16,17] for higher metal thickness. The gold material dispersion also brings contribution to the effective supermode index variation.

2.2. Dielectric permittivity variation with filling factor

The previous example has shown the validity of the (M-G) effective medium model for the case of a low filling factor MMs layer. Increasing the filling factor would obviously result in an adjacent CWs interaction enhancement that could alter the validity of M-G approximation. To verify the M-G approximation validity for higher filling factors, we vary the separation distance between CWs along both the longitudinal and transverse direction.

The results obtained at normal incidence for 200 \times 50 \times 10nm CWs with electric field orientation along the longitudinal axis are shown Fig. 2. In this example the filling factor variation is obtained by changing the transverse separation between adjacent CWs. For better viewing the displayed results represent the effective permittivity normalized by the filling factor: $\epsilon_{\text{norm}} = \epsilon_{\text{eff}} / p$.

As it can be seen, the normalized permittivity is little dependent on the filling factor. For both real and imaginary part the maximal variation of permittivity is less than 16%, while the filling factor variation attains 450%. The shift of the resonance toward higher frequencies with the increase of the filling factor is in agreement with similar MMs structures reported in [18]. This shift is due to the

enhancement of coupling between CWs by dipolar interaction. As it will be shown in the following, the variation of the normalized permittivity would be even lower without the frequency shift.

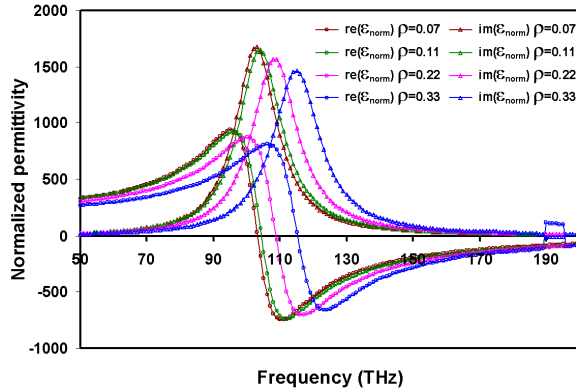


Figure 2: Real and imaginary parts of normalized MM permittivity spectral characteristics for different filling factors. Metal thickness 10nm.

The relative independence of the normalized permittivity is conserved when the variation of the filling factor is performed in a different manner. This point was verified for filling factor variation obtained by changing the longitudinal separation distance or the width of the CWs, the rest of parameters being fixed. Similar behavior holds also for higher metafilm thicknesses. Note also the high values of normalized permittivity exceeding 1000. Even for a filling factor of 10% this means an effective index around 10 at resonance.

2.3. Single metafilm optical length study

Genuine MMs effective parameters have to be independent of the MMs thickness. For the microwave domain this condition is readily verified by varying the number of MMs layers. A convergence of the retrieved MMs effective parameters is expected with the increase of the number of layers. In the case of a single metafilm layer this means that effective parameters have to be independent of the metal thickness. The equivalent condition is to have a linear variation of the optical length with h .

As for the previous examples CWs length is 200nm and width is 50nm while normal incident light electric field orientation is along the longitudinal axis. The refractive index used to calculate the optical length corresponds to the maximal value of the effective index at the resonance frequency. As for the permittivity, its value is also normalized by the filling factor.

The variation of the optical length (normalized by the filling factor) as a function of the thickness h for different CWs densities is shown Fig. 3a. The displayed results show that the variation of the optical length with metal thickness is approximately linear for a thin metal. Strong deviations from linearity occur for metal thicknesses above 50nm, especially for higher filling factors.

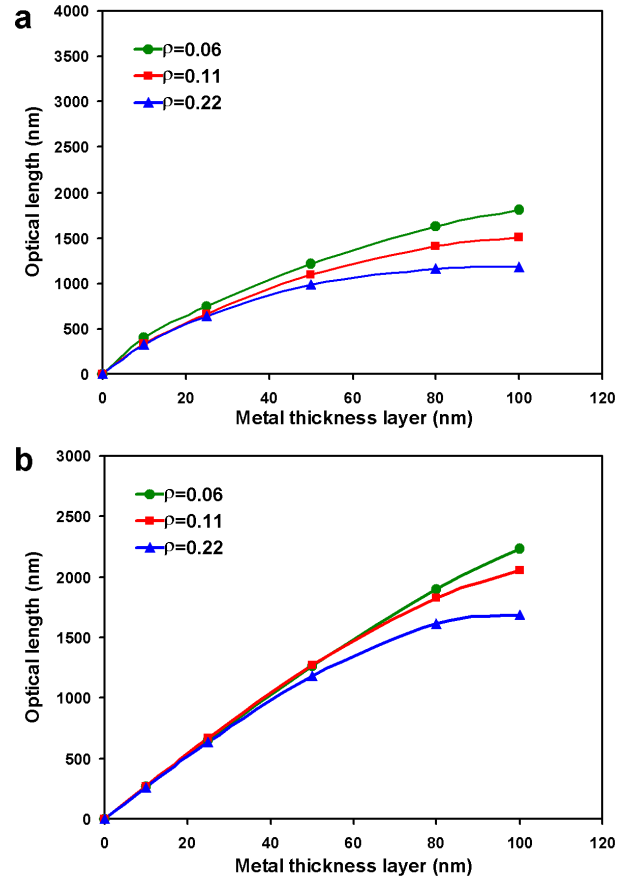


Figure 3: (a) Normalized by filling factor optical length for different CWs densities. b) Same as (a) for 148THz fixed resonance frequency using tuned CWs.

To understand the deviation from linear dependence we compare the spectral characteristics of the normalized permittivity for different MMs thickness. The results corresponding to 10, 25 and 50nm MMs thickness are represented Fig. 4a. The shift of the resonance frequency and permittivity variation are much more important as compared to the case of filling factor variation shown Fig. 3.

To separate thickness and frequency contributions, the length and width of 10 and 50nm thick CWs was tuned to shift the resonance to 148THz while keeping the same filling factor. For 10nm thick CWs this was achieved by changing the length to 138nm, the width to 72nm and having same unit cell size of 300×300nm. A similar procedure was applied to the 50nm thick MMs. For this case the CWs length and width are 245×41nm for a 300×300nm unit cell.

The normalized permittivities for CWs having a resonance at 148THz are represented Fig. 4b. The variation of the normalized permittivity is less than 12% in this case, while it attains 248% for the case corresponding to Fig. 4a. It thus appears that a frequency shift brings a significant contribution in the change of the metafilm effective parameters.

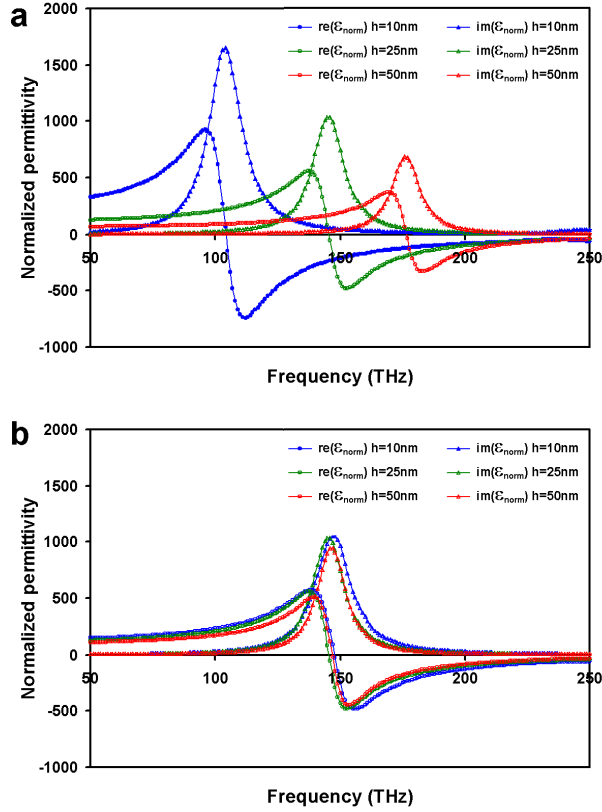


Figure 4: (a) Real and imaginary parts of normalized MM permittivity spectral characteristics for different metafilm thickness. (b) Same as (a) for 148THz fixed resonance frequency using tuned CWs.

The optical length determined for the case of a resonance frequency fixed to 148THz using CWs tuning procedure is shown Fig. 4b. The dependence is much more linear in this case, especially when the filling factor is low. This result further proves the validity of the M-G effective medium model applied to a single metafilm layer.

2.4. Metafilm oblique incidence s polarization behavior

The last point of our analysis concerns the metafilm effective medium behavior under oblique incidence. For p polarization the homogeneous layer approximation is not valid because of the anisotropy of the CW properties with respect to the electric field orientation. For the time being there is no reliable analytical anisotropy retrieval procedure that would allow an appropriate treatment of this case. For this reason our analysis is mainly limited to the case of s polarization, while some discussion concerning the possible implementation of the retrieval procedure for p polarization is presented in the next section. For the s polarization the electric field orientation along the CWs longitudinal axis doesn't vary with the incidence angle. The configuration corresponding to this case is sketched Fig. 5.

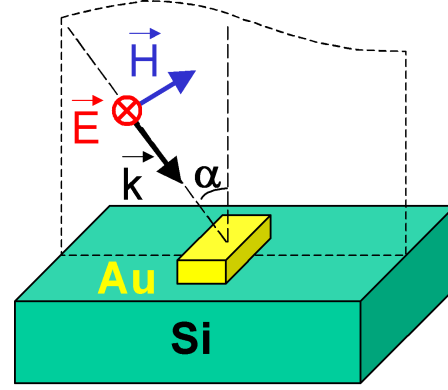


Figure 5: Sketch of s polarization oblique incidence configuration.

The reflection and transmission spectra computed for different angles of incidence are shown in Fig. 6a.

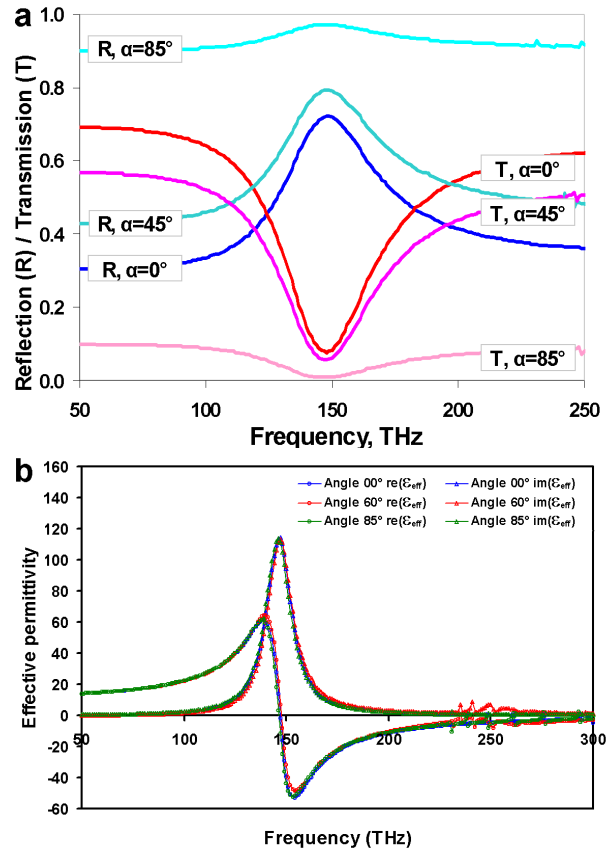


Figure 6: a) Reflection and transmission spectra of single metafilm layer for s polarization different incidence angles. b) Real and imaginary parts of effective MM permittivity spectral characteristics for s polarization different incidence angles.

The plotted results correspond to $200 \times 50 \times 25\text{nm}$ CWs with 11% filling factor. It can be observed that in accordance with Fresnel reflection coefficients, the

reflectivity increases with the incidence angle. At the same time an apparent decrease of the resonance variation for high incidence angles is observed in transmission and reflection.

To extract the metafilm effective parameters we use the described retrieval procedure. The obtained results represented in Fig 6b show that permittivity and permeability are independent of the incidence angle. It should be noted also that outside the resonance region the effective permittivity and respectively the effective index are not too high for low filling factors. As it can be inferred from the Fig. 6b, at low frequency $n_{\text{eff}} \approx 3.8$, that is not too much higher as compared to Silicon. So at high incidence angles, as those showed in our example, the refraction angle inside the metafilm should substantially deviate from the normal axis. It follows from that the independence of the metafilm effective parameters of the incident angle can not be attributed to the near normal axis propagation as it was suggested in [19] were split ring resonators (SRRs) single metafilm was investigated for different incidence angles in the THz spectral domain.

The presented results show that for the particular investigated geometry, when the electric field is oriented along the main MMs symmetry axis, the metafilm behavior is fully analogous to that of a homogeneous layer. The thickness of this layer is that of the deposited metal.

2.5. Full anisotropic characterization

While there is no reliable analytical way to perform a retrieval of the anisotropic dielectric tensor in the case of the p polarization (Fig. 7), another approach can be followed, in which the full permittivity and permeability tensors are retrieved either through brute-force search or heuristic methods.

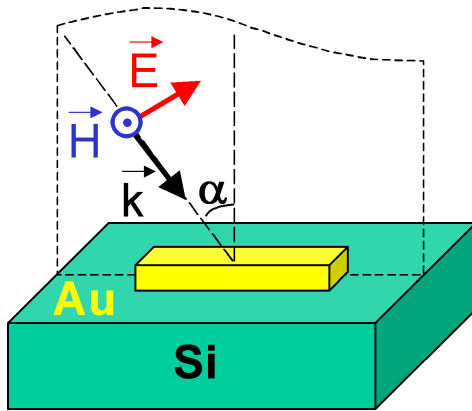


Figure 7: Sketch of p polarization oblique incidence configuration.

To do this, one only needs to know how to solve the direct problem, which is the optical response of an anisotropic slab [20] with known dielectric and permittivity tensors. The inverse problem – retrieving the tensors from known reflection and transmission coefficients – can be

solved by trial and error, through the implementation of an evolutionary search algorithm.

If the tensors are assumed to be diagonal – which is reasonable given the geometry of the structure presented here – the retrieval can be done in two steps: first the components of the tensors which are parallel the substrate are retrieved from result computed for normal incidence, then the tensor components perpendicular to the substrate are retrieved from results computed for oblique incidence. It is one of the future directions of our work.

In the case where the tensors are not diagonal, a similar procedure can be applied, first by retrieving only the components related to the plane parallel to the substrate, and then by computing the remaining components using several different angles of incidence and several polarization. In this case, the retrieval of the optical parameters of the material can be seen as a constrained multi-objective optimization problem.

3. Summary and conclusions

The aim of the present work was to investigate the possibility to describe single metafilm layer behavior formed by an array of CWs as an effective medium. It has been shown that for the particular investigated geometry, when the electric field is oriented along the main MMs symmetry axis, the metafilm behavior is indeed analogous to that of a homogeneous layer. The thickness of this layer is that of the deposited metal. The validity of this conclusion was verified with respect to a number of criteria consistent with the Maxwell-Garnett effective medium model.

It was shown namely that outside the resonance region the magnetic permeability $\mu \approx 1$ and that in accordance with the M-G approximation the effective permittivity is proportional to the filling factor of the MMs. It was found that for small metal thickness and filling factors the metafilm optical length is proportional to the metal thickness. The linearity of the optical length with metal thickness turns to be greatly improved when considering tuned MMs having the same resonance frequency.

Finally, for the polarization perpendicular to the incidence plane the metafilm permittivity is independent of the incident angle.

The generalization of this approach to the case of in-plane polarization was considered, and a study of this case is soon to be submitted [21].

Acknowledgements

This work was supported by the French National Research Agency (ANR Metaphotonique, contract number 7452RA09) and the Champagne-Ardenne region.

References

- [1] V. G. Veselago, "The electrodynamics of substances with simultaneously negative values of permittivity and permeability," *Sov. Phys. Usp.* 10, 504, 1968.
- [2] J.B. Pendry, "Negative refraction makes a perfect lens," *Phys. Rev. Lett.* 85, 3966, 2000.
- [3] X. Chen, T. M. Grzegorzczak, B. I. Wu, J. Pacheco, and J. A. Kong, "Robust method to retrieve the constitutive effective parameters of metamaterials," *Phys. Rev. E* 70, 016608, 2004.
- [4] T. Driscoll, D. N. Basov, W. J. Padilla, J. J. Mock and D. R. Smith, "Electromagnetic characterization of planar metamaterials by oblique angle spectroscopic measurements," *Phys. Rev. B* 75, 115114, 2007.
- [5] J. Zhou, T. Koschny, M. Kafesaki, and C. M. Soukoulis, "Negative refractive index response of weakly and strongly coupled optical metamaterials," *Phys. Rev. B* 80, 035109, 2009.
- [6] C. Menzel, C. Rockstuhl, T. Paul, and F. Lederer, "Retrieving effective parameters for metamaterials at oblique incidence," *Phys. Rev. B* 77, 195328, 2008.
- [7] C. R. Simovski, "On electromagnetic characterization and homogenization of nanostructured metamaterials," *J. Opt.* 13 013001 (2011).
- [8] S. Zhang, W. Fan, N. C. Panoiu, K. J. Malloy, R. M. Osgood, and S. R. J. Brueck, *Phys. Rev. Lett.* 95, 137404, 2005.
- [9] B. Kanté, A. de Lustrac, J.-M. Lourtioz, "Optical metafilms on a dielectric substrate," *Phys. Rev. B* 80, 205120 (2009).
- [10] www.ansoft.com/products/hf/hfss/
- [11] A. Taflov, S.C. Hagness. "Computational electrodynamics: the finite-difference time domain method". Artech House antennas and propagation library. Artech House, 2005.
- [12] E. D. Palik, *Handbook of optical constants of solids* (Academic Press, New York, NY 1998).
- [13] A. Lupu, N. Dubrovina, R. Ghasemi, A. Degiron, and A. de Lustrac, "Metal-dielectric metamaterials for guided wave silicon photonics," *Opt. Express* 19, 24746–24761, 2011.
- [14] D. R. Smith, S. Schultz, P. Markos and C. M. Soukoulis, "Determination of effective permittivity and permeability of metamaterials from reflection and transmission coefficients," *Phys. Rev. B* 65, 195104, 2002.
- [15] T. Koschny, P. Markoš, D. R. Smith, and C. M. Soukoulis, "Resonant and antiresonant frequency dependence of the effective parameters of metamaterials," *Phys. Rev. E* 68, 065602(R), 2003.
- [16] D. Sarid, "Long-range surface-plasma waves on very thin metal films," *Phys. Rev. Lett.* 47, 1927–1930, 1981.
- [17] P. Berini, "Long-range surface plasmon-polaritons," *Adv. Opt. Photonics* 1, 484–588, 2009.
- [18] D. Weber, P. Albella, P. Alonso-González, F. Neubrech, H. Gui, T. Nagao, R. Hillenbrand, J. Aizpurua, and A. Pucci, "Longitudinal and transverse coupling in infrared gold nanoantenna arrays: long range versus short range interaction regimes," *Opt. Express* 19, 15047-15061, 2011.
- [19] C. Menzel, R. Singh, C. Rockstuhl, W. Zhang, and F. Lederer, "Effective properties of terahertz double splitting resonators at oblique incidence," *J. Opt. Soc. Am. B* 26, B143-B147, 2009.
- [20] D. W. Berreman. "Optics in stratified and anisotropic media: 4x4 – matrix formulation" *J. Opt. Soc. Am.* 62, 502-510, 1972.
- [21] L. O. Le Cunff, N. Dubrovina, A. Vial, A. De Lustrac, A. Lupu, G. Lerondel, "3D modeling of metamaterials and anisotropic characterization" (to be submitted).